# IMECE2003-55424

## Autonomous Landing for Indoor Flying Robots Using Optic Flow

William E. Green, Paul Y. Oh, Keith Sevcik and Geoffrey Barrows
Drexel University, Philadelphia PA and Centeye Inc., Washington DC
Email: [weg22, paul.yu.oh, kws23]@drexel.edu and geof@centeye.com

### Abstract

*Urban environments are time consuming, labor intensive and possibly dangerous to safe guard. Accomplishing tasks like bomb detection, search-and-rescue and reconnaissance with aerial robots could save resources. This paper describes a prototype called CQAR: Closed Quarter Aerial Robot, which is capable of flying in and around buildings. The prototype was analytically designed to fly safely and slowly. An optic flow microsensor for depth perception, which will allow autonomous takeoff and landing and collision avoidance, is also described.*

## 1  Introduction

More often homeland security missions occur in closed quarters which are spacious but enclosed urban environments like stadiums, underground parking lots, subway tunnels and train stations. Common missions include bomb detection, reconnaissance and surveillance. For disaster mitigation or military operations, missions include search-and-rescue, and bomb damage assessment. All of these missions risk human life, are time consuming and often demand large allocations of resources. Employing robots for such missions has been attempted for decades with marginal success [8]. Recent experiences at the World Trade Center and in Afghanistan underscore that ground based robots often cannot overcome rock piles, climb stairs quickly or function effectively without a tether [2].

Aerial robots, capable of flying in closed quarters, may be an alternative to wheeled or tracked robots. Flying permits traveling down tunnels or halls quickly while not inhibited by stairs (see Figure 1). Milestones in aerial robotics have been achieved have been recently achieved using sensor suites that include GPS, inertial measurement units, laser altimeters, ultrasound and computer vision to perform missions like terrain-following, base station keeping and automated landing. These successes are however limited to outdoor flying. For example, GPS does not provide the re-



Figure 1: Closed quarters like this multi-floor atrium are enclosed but spacious for aerial robots.

quired precision for operation in closed quarters and GPS signals are easily jammed. Also vision-based methods that reference the horizon (Pipitone et al [10]) are also inappropriate indoors. Furthermore, closed quarters often demands being small and must fly slowly and safely in order to maneuver through halls and tunnels. Conventional fixed-wing micro aerial vehicles which typically have a 6-inch wing span but fly at 20 miles per hour [5]. Small rotorcraft, including quad-rotors [7], are even more difficult to fly than conventional model helicopters. These aircraft are inherently unstable and hence autonomy for indoor flying will remain challenging. Lighter-than-air vehicles, like blimps, fly slowly and can hover [13]. Buoyancy however is proportional to volume and hence blimps are often too large to fit through doors. Recently flapping has been investigated as a flight mode but results have been limited to lab demos while tethered to a table top power supply [3]. The net effect is the design methods for flying robots outdoors do not apply well in closed quarters.

Our vision is to design a flying robot we call CQAR: *Closed Quarter Aerial Robot* (pronounced "seeker"). Designing such a robot has become possible re-

cently due to advances with Lithium-polymer batteries, lightweight materials like carbon fiber rods, small but powerful embedded micros, low-power sensors and high-torque miniature motors. Recently, Nicoud and Zufferey at EPFL in Lausanne Switzerland debuted an indoor aerial robot prototype [9]. Their current version does not feature any sensors but does use Bluetooth to control the vehicle from user input to a laptop computer. This paper formulates a design prototype for a closed quarter aerial robot and documents our progress in autonomous take and landing using optic flow microsensors. Section 2 describe the multidisciplinary design optimization used to understand design tradeoffs in flight structure, aerodynamics, task performance and sensor selection. Section 3 reveals the resulting prototype along with some results in using carrying a wireless camera. Section 4 discusses the capabilities of using optic flow microsensors for flight control and autonomous takeoff and landing. Section 5 concludes and outlines near-future goals.

## 2 Optimal Design Matrix

A closed quarter aerial robot demands understanding how aerodynamics, sensor suite integration and task influence design. Towards this a multi-disciplinary design optimization (MDO) matrix (Grasmeyer, Keennon [5]) is very helpful. The MDO method originated in the automobile industry and has evolved into an invaluable discipline that supplies engineers with techniques to move engineering system design closer to optimal. Inputting some initial components into a design matrix will yield the most applicable platform and its corresponding equations of motion.

Each design variable used has a large impact on platform selection (see Figure 2). The parameters that make up the design matrix include initial variables $X_I$, velocity variables $X_V$, size variables $X_S$, payload variables $X_P$, and hover variables $X_H$. The initial variables determine the mission type and include parameters such as environment (closed quarter, outdoors or both), desired tasks (search and rescue or reconnaissance), expendability, vertical takeoff and landing requirements, and stealthy operation. The velocity parameters are used to establish speed range capabilities. The size variables represent the platforms maximum characteristic length as well as propeller diameter. This will conclude whether or not the vehicle can fit through small openings like doorways. Payload variables determine the weight and dimensions of the designed sensor suite. The hover parameters assess



Figure 2: Design matrix input parameters

whether or not there is a requirement and also the endurance of the hover. Common input parameters such as flight endurance, range or propeller geometry were not selected in this design matrix because such parameters can be manipulated once the optimal platform is selected.

Based on the input parameters specified above, the program executes a series of commands to generate the most suitable aerial platform and its corresponding equations of motion (see [6] for more details). The result of these inputs suggest a fixed-wing design.

## 3 Fixed-Wing Aircraft

Fixed-wing aircraft design has a long history and governed by the principle that an aircraft's weight is proportional to its cruise velocity

$$ W = \frac{1}{2}\rho V^2 S C_L \qquad (1) $$

Therefore, the lighter the aircraft, the lower the velocity requirements to maintain steady and level flight. Lower velocity requirements also correspond to higher maneuverability, which is crucial for closed quarters. The four forces of flight on a fixed wing aircraft are lift $L$, drag $D$, thrust $T$ and weight $W$ and are sketched
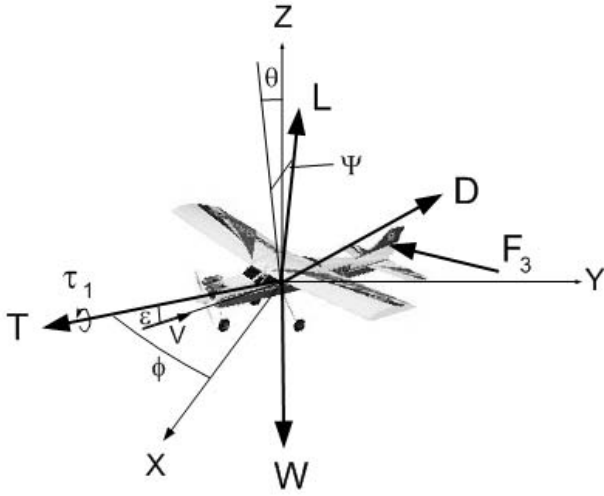
Figure 3: Free-body diagram of fixed-wing vehicle

in Figure 3. $\theta$, $\Psi$ and $\phi$ are the rigid body rotations about the $x$, $y$ and $z$ axes respectively. $\tau_1$ is the propeller's reaction force and the angle between the free-stream velocity and the thrust vector is $\varepsilon$. The four forces of flight and the moment of inertia $J$ are about the airplane's center of gravity. Thus, the Newtonian equations of motion for a fixed wing aircraft in three-dimensional space are:

$$m_x a_x = T \cos\theta \cos\Psi \cos\phi - D \cos\varepsilon \cos\theta \cos\Psi \cos\phi$$
$$- L \cos\theta \sin\Psi \cos\phi + F_{3_x}$$
$$m_y a_y = -T \cos\theta \cos\Psi \sin\phi + D \cos\varepsilon \cos\theta \cos\Psi \sin\phi$$
$$- L \sin\theta \cos\Psi \cos\phi + F_{3_y}$$
$$m_z a_z = T \cos\theta \sin\Psi \cos\phi - D \cos\varepsilon \cos\theta \sin\Psi \cos\phi$$
$$- W + L \cos\theta \cos\Psi \cos\phi + F_{3_z}$$

$$
\begin{aligned}
J_x \dot{\omega}_x &= \tau_{1_x} + F_{3_z} l_y + F_{3_y} l_z \\
J_y \dot{\omega}_y &= \tau_{1_y} + F_{3_z} l_x + F_{3_x} l_z \\
J_z \dot{\omega}_z &= \tau_{1_z} + F_{3_x} l_y + F_{3_y} l_x
\end{aligned}
$$

It can be seen from the equations above that $L = W$ and $T = D$ during cruise flight ($a_x = a_y = a_z = \theta = \Psi = \phi = 0$).

## 3.1 CQAR Prototype

Employing fixed-wing aircraft design, a prototype with a 46 $cm$ wing span and 26 $g$ mass (about 3 U.S. quarter coins) was constructed. The resulting vehicle can carry a 14 $g$ sensor payload and navigate in a $10 \times 10$ $m^2$ area (about 1/3 the size of a basketball court) when flying at a maximum speed of 2 $m/s$ (about the speed of a slow jogging person).
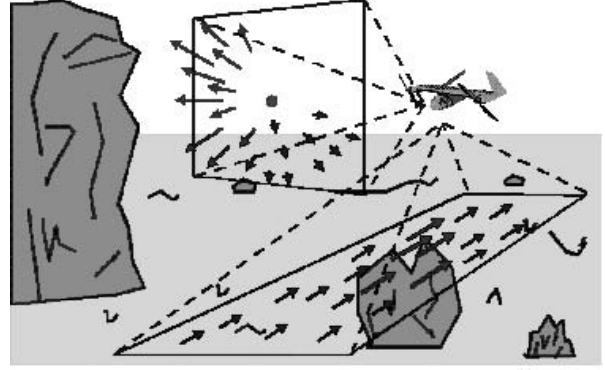


Figure 5: Optic flow as seen by aerial robot flying above ground.

The fuselage and airfoil frame were constructed out of carbon fiber rods with a 3 $\mu m$ mylar covering, while the tail is made from mylar covered balsa wood. With a payload capacity of 14 $g$, the aircraft can carry a light-weight mini wireless camera and power supply as shown in Figure 4 (left). The middle photo is a frame captured by the on-board camera while flying in the atrium (Figure 1). A table can be identified, but the image is noisy. For comparison, the actual table is depicted in the right photo. The noise is due to both interference from the university's 802.11b wireless network and the wireless camera's poor performance. We are currently testing more robust light-weight wireless cameras.

## 4 Optic Flow for Navigation

Collision avoidance is especially crucial in navigating through closed quarters. Infrared proximity sensors and ultrasonic sensors are often used by ground-based mobile robots to steer around obstacles [4]. The CQAR prototype has a minimum flying speed of 2 $m/s$ and a turning radius of about 2.5 meters. To avoid large obstacles, it is preferable to detect them and initiate a turn at least two turning radii away (5 meters). This distance is generally out of range or accuracy of small, lightweight ultrasonic or infrared sensors. Processing of images captured by an aerial robot's on-board camera has been performed on outdoor aerial robots. Common methods exploit image features provided by the horizon [10] or flying field [12] which are both absent in closed quarters. The net effect is that conventional sensors and methods, although successful outdoors, have limitations indoors and thus demand alternative approaches. Insects make heavy use of vision, especially optic flow, for
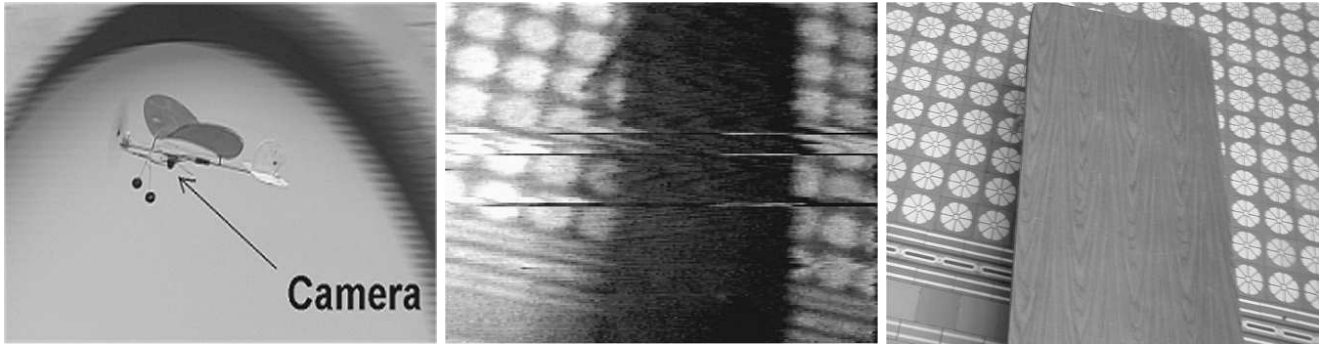
Figure 4: An on-board wireless camera mounted on the flying prototype (left) can acquire video and transmit images (middle). Such images, although noisy, compare well with regular cameras (right).
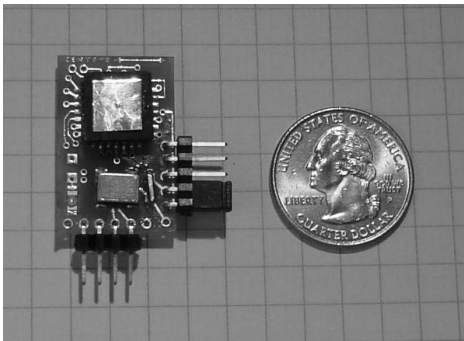


Figure 6: mixed-mode VLSI optic flow microsensor is slightly bigger than a US quarter.

perceiving the environment. Optic flow is essentially the apparent visual motion experienced by an insect as it travels through the environment. Objects that are close will tend to appear to move faster than objects that are far away, and objects with which the insect are on a collision course will tend to appear as if they are rapidly increasing in size. Figure 5 depicts optic flow as it might be seen by an aerial robot traveling a straight line above the ground. The robot can estimate its height from the optic flow in the downward direction. The robot is able to detect the presence of obstacles by expansion in the forward direction. Through the use of multiple optic flow sensors, it is possible to estimate the aircraft's self-motion with respect to the Earth, including rotation information and sideslip.

Optic flow has been applied to outdoor flying vehicles for terrain-following and altitude control [11]. For smaller sized vehicles, Centeye has developed the *Ladybug* optic flow microsensor, shown in Figure 6. The resulting sensor is composed of two parts: a mixed-mode "vision chip" images the environment and performs low-level processing using analog VLSI circuitry. Then an off-the-shelf microcontroller performs mid- and high-level processing using standard digital techniques. The resulting sensor, including optics, imaging, processing, and I/O weighs 4.8 grams. This sensor grabs frames up to 1.4 $kHz$, measures optic flow up to 20 $rad/s$, and functions even when texture contrast is just several percent. Details of the current sensor are unpublished, but earlier generations are described in [1]. Such Ladybug sensors have been used to provide 1-meter outdoor RC aircraft with reliable autonomous altitude hold, terrain following, and obstacle detection.

## 4.1 Autonomous Takeoff and Landing (ATOL) Control

Optic flow can be used to autonomously land an aerial robot in closed quarters. To simplify this task, the rotational component of optic flow arising from changes in aircraft pitch are assumed smaller than the translational component. Srinivasan observed that honeybees land by keeping the optic flow on the landing surface constant ($v/d$, where $d$ is the altitude). Mimicking this behavior demands the fixed-wing aircraft decrease forward speed in proportion to altitude. Autonomous takeoff is simpler and can be achieved by applying full throttle with elevator deflection.

The optic flow control system block diagram and flow chart are shown in Figures 7 and 8 respectively. When approaching a landing, an embedded microprocessor, or controller, will take an initial reading from the optic flow sensor (see Figure 9) and set that as the desired value, $o_i(t)$. The controller will then implement a function to gradually throttle down the motor while continuing to take readings throughout the
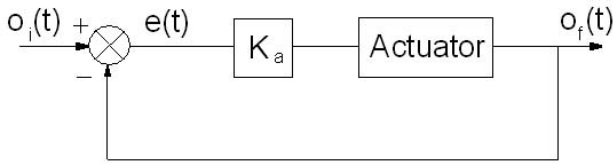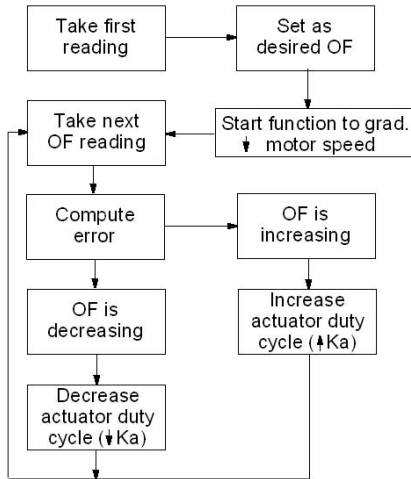
Figure 7: Optic flow control system block diagram.



Figure 8: Flow chart of how control system operates.

landing process. The error, $e(t)$, is computed between the desired and actual values, $o_i(t)$ - $o_f(t)$. When the optic flow on the landing surface becomes larger than the desired optic flow, the error is negative and two conditions are possible. One, the forward velocity, $v$, could be significantly increasing which is not possible based on our motor function. Two, the altitude, $d$, can be decreasing at a faster rate than $v$. Here, the controller will raise the PWM duty cycle, based on the error magnitude and proportional constant, $K_a$, to the elevator's actuator to deflect the control surface upwards. The other possibility is that the optic flow could start to dip below the desired level causing the error to be positive. The two possible cases that arise here are one, $d$ is increasing but again this is not practical while in landing mode and two, $v$ is decreasing faster than $d$. In this case, the controller will need to decrease the PWM duty cycle and again send the output to the actuator. After a control sequence has been implemented to force the optic flow back to the desired value, the elevator should be reset to its initial settings (i.e. actuatorDuty = neutral).
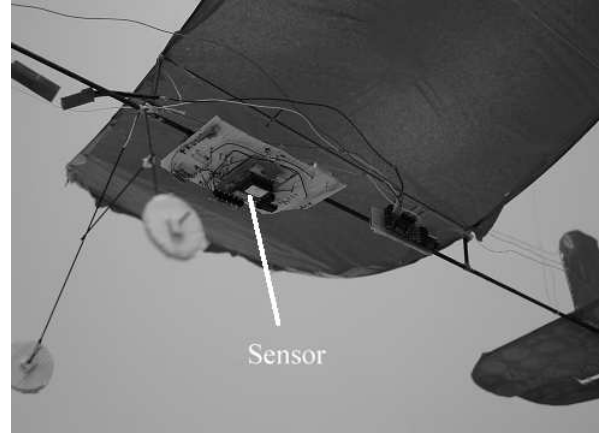


Figure 9: An optic flow sensor suite is used to achieve autonomous takeoffs and landings.

## 4.2 Landing Baseline Metrics

To test the success of our ATOL control system, data was gathered from an expert human piloted landing inside a basketball gymnasium (see Fig. 10). Landing metrics such as force of ground impact, or lack of bounce, overshoot or undershoot from a landing target (measured from c.g.), distance from runway centerline (c.g.), and maintaining pose throughout the landing sequence (i.e. keeping aircraft fuselage in line with centerline and at a constant angle-of-attack) were formulated. Because of the payload constraints, we were not able to equip our plane with force sensors or gyros to measure the force of ground impact or pose. Instead, we rated these categories on a scale of 1 to 10 with 10 being no bounce from ground impact and constant pose throughout landing sequence.

As expected, the best results were seen in the centerline category because it extends beyond the landing target. The significant error in the human's ability to hit the target resulted from the force of impact. That is, the plane was lined up to hit the target on most trials, but would stop substantially short if it hit the ground hard. In contrast, it would overshoot the target if it contacted the ground so lightly that it became airborne again for a few seconds. The aircraft's pose was affected by the "bang bang" control method implemented by the human. The motor was cut in the initial stage of the landing sequence so that the aircraft could glide to a landing. If it appeared the aircraft was going to undershoot the target, the human quickly increased and then decreased the throttle to give just enough thrust to hit the target. This type of control, however, proved to cause significant changes
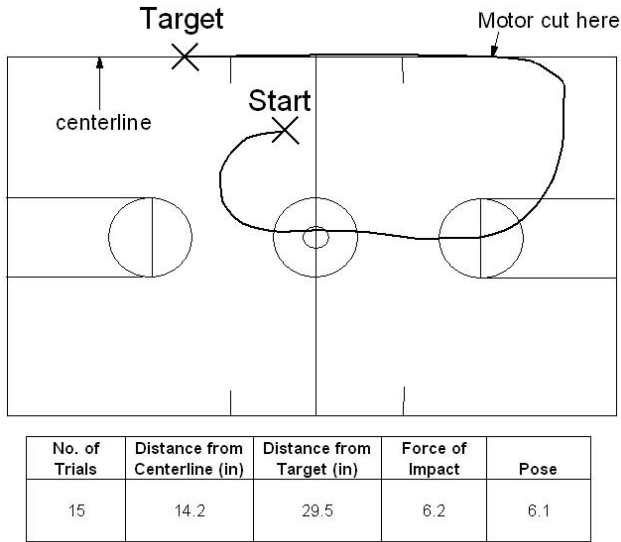
Figure 10: Top: Path taken by human to land aircraft. Bottom: Results based on formulated metrics

in the aircraft's attitude and is evidenced by a low score in the pose category. While the human could "see" the aircraft's pose changing and make necessary adjustments, our control system cannot. Therefore, we felt to achieve a better overall score then the human, an autonomous landing should be carried out by slowly decreasing the motor (starting at the point where the human cuts the motor) while controlling the elevator to maintiain pose.

## 5 Conclusions and Future Work

Closed quarters which are enclosed but spacious areas like warehouses, stadiums, underground parking lots and tunnels, are time consuming and labor intensive to patrol and safe keep. A robot designed to fly in closed quarters and deliver situational awareness would benefit homeland security, disaster mitigation and military operations. Applications could include biochemical detection, search-and-rescue and reconnaissance. This paper presented a working prototype based on output from a optimization matrix that parameterized design variables. The resulting closed quarter aerial robot (CQAR) can fly safely and slowly in an area as small as $10 \times 10$ square meters and deliver wireless video with its on-board camera. Optic flow, often used in insect navigation, can be captured using VLSI hardware. This paper describes how such a sensor can be used as well as the results for human targeted landing.

## References

[1] Barrows, G., Neely, C., "Mixed-mode VLSI Optic Flow Sensors for In-flight Control of a Micro Air Vehicle", *Proc. SPIE*, 4109 pp. 52-63, 2000.

[2] Blitch, J., "World Trade Center Search-and-Rescue Robots", Plenary Session *IEEE Int Conf Robotics and Automation*, Washington D.C., May 2002.

[3] Fearing, R., et al, "Wing Transmission for a Micromechanical Flying Insect", *IEEE Int Conf Robotics and Automation*, San Francisco pp. 1509-1516, April 2000.

[4] Flynn, A.M., "Combining Sonar and Infrared Sensors For Mobile Robot Navigation", *Int. Journal of Robotics Research*, pp. 5-14, December 1988.

[5] Grasmeyer, J.M., Keennon, M.T., "Development of the Black Widow Micro Air Vehicle", *39th AIAA Aerospace Sciences Meeting and Exhibit*, Reno, NV, Jan. 2001.

[6] Green, W.E., Oh, P.Y., "An Aerial Robot Prototype for Situational Awareness in Closed Quarters", *IEEE/RSJ Int Conf on Robots and Systems*, Las Vegas, NV, Nov. 2003 (in press).

[7] Hamel, T.; Mahony, R., Chriette, A., "Visual Servo Trajectory Tracking for a Four Rotor VTOL Aerial Vehicle", *IEEE International Conference on Robotics and Automation (ICRA)*, Washington, D.C., pp. 2781-2786, 2002.

[8] Murphy, R., et al, "Mobility and sensing demands in USAR", *IEEE Industrial Electronics Conference (IECON)*, V1, pp. 138-142, 2000.

[9] Nicoud, J.D., Zufferey, J.C., "Toward Indoor Flying Robots", *IEEE/RSJ Int Conf on Robots and Systems*, Lausanne, pp. 787-792, October 2002.

[10] Pipitone, F., Kamgar-Parsi, B., Hartley, R., "Three Dimensional Computer Vision for Micro Air Vehicles", *Proc. SPIE 15th Aerosense Symposium*, Conf. 4363, Enhanced and Synthetic Vision 2001, Orlando Florida, April 2001.

[11] Srinivasan, M.V., Chahl, J.S., Weber, K., Venkatesh, S., Nagle, M.G., Zhang, S.W., *Robot Navigation Inspired By Principles of Insect Vision* in Field and Service Robotics, A. Zelinsky (ed), Springer Verlag Berlin, NY 12-16.

[12] Saripalli, S., Montgomery, J.F., Sukhatme, G.S., "Vision-based Autonomous Landing of an Unmanned Aerial Vehicle", *IEEE International Conference on Robotics and Automation (ICRA)*, Washington, D.C., pp. 2799-2804, 2002.

[13] Zhang, H., Ostrowski, J.P., "Visual Servoing With Dynamics: Control of an Unmanned Blimp", *IEEE International Conference on Robotics and Automation (ICRA)*, Detroit, pp. 618-623, 1999.